

# Cross-correlation frequency-resolved optical gating by molecular alignment for ultraviolet femtosecond pulse measurement

Peifen Lu, Jia Liu, Hao Li, Haifeng Pan, Jian Wu,<sup>a)</sup> and Heping Zeng<sup>b)</sup>

State Key Laboratory of Precision Spectroscopy, East China Normal University, Shanghai 200062, People's Republic of China

(Received 27 April 2010; accepted 15 July 2010; published online 9 August 2010)

We experimentally demonstrate a molecular-alignment-based cross-correlation frequency-resolved optical gating technique for ultraviolet femtosecond pulse measurement, which use laser-induced impulsive alignment of gaseous molecules as the gate function instead of the phase-matched frequency mixing process in a nonlinear crystal. The spectrogram measurements and retrieving results of the intensity and phase of the second and third harmonic pulses centered at 400 and 267 nm are presented. © 2010 American Institute of Physics. [doi:10.1063/1.3478008]

The frequency-resolved optical gating (FROG) technique is one of the most popular and robust methods for ultrashort laser pulse characterization,<sup>1-4</sup> which involves an experimental apparatus to create a spectrogram of a target pulse resulting from its convolution with a gate function and a retrieval algorithm. For different particular applications, a variety of geometries were developed for FROG measurements, such as the polarization gating,<sup>5</sup> self-diffraction,<sup>6</sup> second harmonic (SH) generation,<sup>7</sup> third harmonic (TH) generation,<sup>8</sup> and transient grating<sup>9</sup> geometries. However, the conventional FROG technique is inefficient for the circumstances when the pulses are very weak or the wavelengths lie in the ultraviolet (UV) region. In order to solve this problem, a cross-correlation FROG (XFROG) technique was suggested,<sup>10</sup> where a fully characterized intense laser pulse was used as the gate function and the spectrogram was obtained through the nonlinear frequency conversion process in a nonlinear crystal. By using a difference-frequency generation XFROG, a weak ultrashort UV pulse at 400 nm was characterized.<sup>11</sup> Since a nonlinear frequency mixing crystal is required, the ultrashort pulse measurement is restricted by the achievable phase-matched spectral bandwidth, group-velocity mismatch, frequency conversion efficiency, transparent spectral range of the crystal, and material dispersion induced broadening of the pulses. A linear process with an ultrafast gate should be better used for ultrashort UV pulse measurements. Impulsive alignment of gaseous molecules and its periodic revivals could function as well-characterized gates,<sup>12,13</sup> since the prealigned linear molecules experience, respectively, increased and decreased refractive indexes for laser field components parallel and perpendicular to the molecular axis, which can thus be treated as a transient wave plate. Accordingly, the polarization state of a properly matched ultrashort laser pulse is rotated as long as its input polarization differs from the direction parallel or perpendicular to the molecular alignment direction.<sup>14</sup>

In this paper, we demonstrate that the impulsively aligned linear molecules as a transient gate function can be used to measure the temporal envelope and phase of an ultrashort UV pulse based on the XFROG technique. As compared with the conventional nonlinear frequency mixing

based FROG geometries, the molecular-alignment-gated XFROG (M-XFROG) makes no use of any nonlinear crystals for nonlinear frequency conversion. Since no phase-matching is required, the M-XFROG can be in principle used to characterize ultrashort laser pulses at any wavelengths in the transparent range of the gases. It also shows distinct features such as low dispersion, spectral narrowing avoidance, weak field intensity measurement, and so forth.

As an instant demonstration, as schematically depicted in Fig. 1(a), an output from an amplified Ti:sapphire laser system (35 fs, 800 nm, and 1 kHz) was split into two following pulses by a beam splitter: one of them was used as the M-pulse for impulsive molecular alignment and the other was used to produce UV test pulses. A SH pulse centered at 400 nm was first generated by a  $\beta$ -barium borate (BBO) crystal (type-I, 29.2°-cut, 200- $\mu$ m-thick). And then a TH pulse at 267 nm was produced by using a second BBO crystal (type-II, 55.4°-cut, 150- $\mu$ m-thick) through frequency summing of the residual fundamental-wave (FW) and the generated SH pulses. The UV pulse was then collinearly

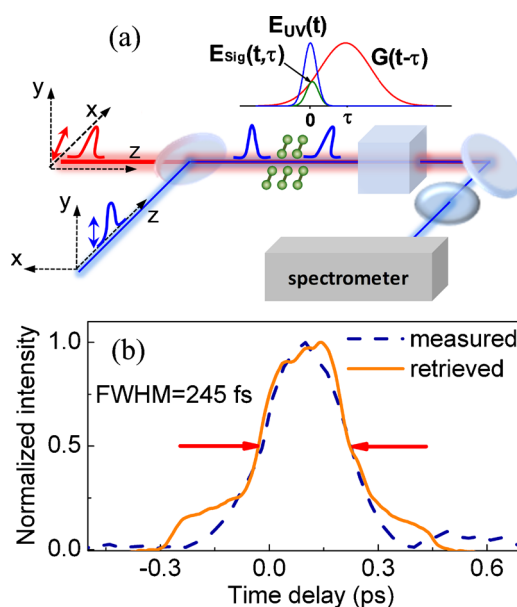


FIG. 1. (Color online) (a) Schematic of an M-XFROG and (b) a slice of the measured molecular alignment signal of air shortly after the M-pulse (navy-dashed line) and the retrieved gate function (orange-solid line).

<sup>a)</sup>Electronic mail: jwu@phy.ecnu.edu.cn.

<sup>b)</sup>Electronic mail: hpzeng@phy.ecnu.edu.cn.

combined with the M-pulse by means of a dichromatic mirror. The change in the polarization state of the input UV pulse by the impulsively aligned molecules was analyzed with a polarizer, whose transmission direction was set to be perpendicular to the input polarization of the UV pulse. The XFROG spectrogram as a transmission after the polarizer analyzer was measured by a spectrometer as a function of the time delay between the transient molecular alignment gate and the UV pulse. In order to have an optimal contrast ratio, the field polarization of the M-pulse was rotated by  $45^\circ$  with respect to the UV pulses. The energies of the M-pulse and SH pulse after the combining mirror were measured to be  $\sim 800$  and  $100 \mu\text{J}$  ( $< 10 \mu\text{J}$  for the TH pulse), respectively.

In general, any gaseous linear molecules of nonzero polarizability anisotropy can be impulsively aligned and used as the transient gate function for the M-XFROG. For the sake of experimental convenience, we used here the diatomic molecules of  $\text{N}_2$  and  $\text{O}_2$  in air. The diatomic molecules were impulsively aligned by the ultrashort FW M-pulse, which then field-free revived with time periods determined by the molecular constants due to the quantum beatings of the excited rotational wave packets. Since the strength of the molecular alignment reached its maximum shortly after the M-pulse excitation owing to the combined contribution of the molecular  $\text{N}_2$  and  $\text{O}_2$ , we used the molecular alignment shortly after the M-pulse excitation as the transient gate function. As shown in Fig. 1(b) (dashed curve), it also exhibited a single peak structure as compared with the other periodic revivals,<sup>13</sup> which consequently led to a clear XFROG spectrogram. The contribution of the instantaneous Kerr effect during the short M-pulse duration to the gate function is small as compared with the molecular alignment. The full width at half maximum (FWHM) of the molecular alignment gate was estimated to be  $\sim 245$  fs. As we will show in what follows, for a given gate function, ultrashort laser pulse with temporal duration much shorter than the gate width could be measured by the M-XFROG.

As schematically shown in Fig. 1(a), as a result of the convolution between the molecular alignment gate and the UV target pulse, the M-XFROG signal in the time domain can be written as  $E_{\text{Sig}}(t, \tau) = E_{\text{UV}}(t)G(t - \tau)$ , where  $E_{\text{UV}}(t)$  is the electric field of the UV pulse and  $G(t - \tau)$  is the gate function. We note that the molecular alignment induced refractive index change serving as the gate function is a real arithmetic quantity, which adds no phase information to the gated slice of  $E_{\text{UV}}(t)$ . This is quite different from the conventional nonlinear frequency mixing based FROG geometries, where the gate function is usually a laser pulse with additional phase modulations. On the other hand, in comparison with the nonlinear frequency mixing process, the polarization change in the target pulse depends linearly on its field intensity, and the measured M-XFROG spectrogram is indeed a linear trace with respect to the target pulse. Meanwhile, the shape of the molecular alignment gate is insensitive to the small fluctuations of the M-pulse. These make the M-XFROG work as a robust technique for ultrashort laser pulse measurement. By spectrally resolving the signal pulse transmitted by the analyzer versus delay, an M-XFROG trace was measured as

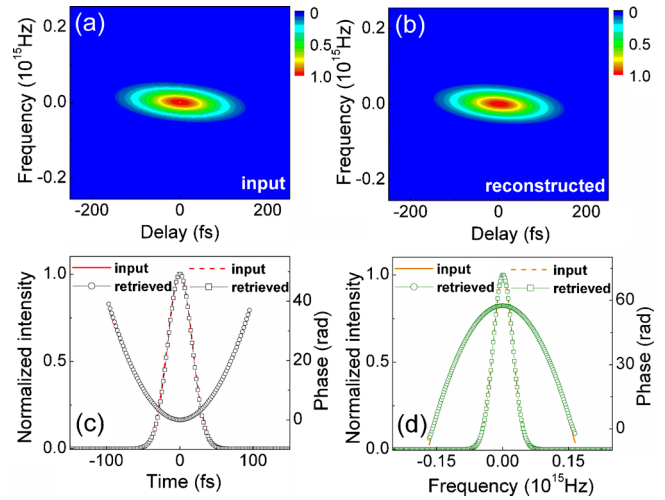


FIG. 2. (Color online) (a) The input M-XFROG trace and (b) the reconstructed FROG trace. (c) The input (solid and dashed red lines) and retrieved (circular and square dark lines) temporal intensity and phase. (d) The input (solid and dashed orange lines) and retrieved (circular and square olive lines) spectral intensity and phase.

$$I_{\text{XFROG}}(\omega, \tau) = \left| \int_{-\infty}^{\infty} E_{\text{UV}}(t)G(t - \tau)\exp(-i\omega t)dt \right|^2. \quad (1)$$

To retrieve the unknown UV pulse  $E_{\text{UV}}(t)$  from the measured XFROG trace, we implemented an iterative Fourier-transform algorithm with a generalized projection method.<sup>15</sup> Briefly, the retrieval procedure was as follows. For the first projection, the trace signal  $E_{\text{Sig}}(t, \tau)$  was constructed as a convolution of a guessed electric field  $E_{\text{UV\_Guess}}(t)$  and the input gate function. It was Fourier transformed to obtain the  $\tilde{E}_{\text{Sig}}(\omega, \tau)$  whose amplitude was then replaced by the square root of the measured XFROG trace  $I_{\text{XFROG}}(\omega, \tau)$ , which was inversely Fourier transformed to have a new trace signal  $E'_{\text{Sig}}(t, \tau)$ . To find the new  $E'_{\text{UV}}(t)$  for next generalized projection, we defined a distance metric

$$Z = \sum_{i,j=1}^N |E'_{\text{Sig}}(t_i, \tau_j) - E'_{\text{UV}}(t_i)G(t_i - \tau_j)|^2. \quad (2)$$

In order to minimize  $Z$  with respect to  $E'_{\text{UV}}(t)$ , the conjugate gradient based Fletcher–Reeves and Polak–Ribiere methods were used with

$$\frac{\partial Z}{\partial \text{Re}[E'_{\text{UV}}(t_k)]} = 2 \sum_{j=1}^N \{ \text{Re}[E'_{\text{UV}}(t_k)][G(t_k - \tau_j)]^2 - \text{Re}[E'_{\text{Sig}}(t_k, \tau_j)]G(t_k - \tau_j) \}, \quad (3)$$

$$\frac{\partial Z}{\partial \text{Im}[E'_{\text{UV}}(t_k)]} = 2 \sum_{j=1}^N \{ \text{Im}[E'_{\text{UV}}(t_k)][G(t_k - \tau_j)]^2 - \text{Im}[E'_{\text{Sig}}(t_k, \tau_j)]G(t_k - \tau_j) \}. \quad (4)$$

The iterative process was repeated until the XFROG trace error reaches an acceptable minimum.<sup>3</sup>

In order to evaluate the validity of the M-XFROG for the ultrashort laser pulse measurement, as shown in Fig. 2(a), we numerically constructed an XFROG trace for an assumed negatively chirped Gaussian pulse of 40 fs (FWHM) and a molecular alignment gate of 200 fs (FWHM). The temporal

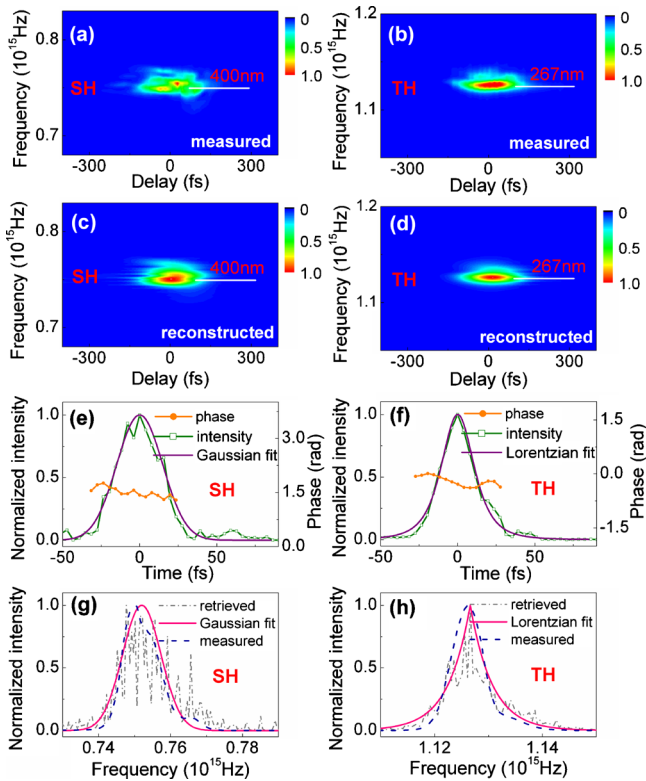


FIG. 3. (Color online) The measured [(a) and (b)] and reconstructed [(c) and (d)] M-XFROG traces of the SH [(a) and (c)] and TH [(b) and (d)] UV pulses. The retrieved temporal profile (square olive line), fitted temporal profile (solid purple line) and phase (circular orange line) of the SH and TH pulses are shown in [(e) and (f)], respectively. The comparisons of the spectral intensity between the measured (dashed royal line) and retrieved (dash-dotted gray line) of the SH and TH pulses are shown in [(g) and (h)], respectively.

intensity and phase of the assumed pulse were then retrieved by the above-mentioned phase-retrieval algorithm. As we can see from Fig. 2, the retrieved XFROG trace [Fig. 2(b)], pulse intensity and phase in the time domain [Fig. 2(c)], and spectral intensity and phase [Fig. 2(d)] agree well with the input ones. The almost perfect agreement between the input and the retrieved pulses clearly indicates the capacity and validity of the M-XFROG technique for ultrashort laser pulse measurement.

The experimentally measured M-XFROG traces for the generated SH and TH pulses are shown in Figs. 3(a) and 3(b), respectively. As compared with the nonlinear frequency conversion based XFROG, here the measured spectrogram was actually the same wavelength as the target pulse. A linear interpolation was applied to create a  $512 \times 512$  pixel trace for the iterative Fourier-transform algorithm. After an iteration of 300 projections, the final XFROG trace errors of  $G=0.0108$  and  $0.0067$  were reached for the SH and TH pulses, respectively. The reconstructed XFROG traces are shown in Figs. 3(c) and 3(d). Figures 3(e) and 3(f) depict the retrieved temporal intensity and phase for the SH and TH

pulses, respectively. The temporal durations of the SH and TH pulses are estimated to be  $\sim 35$  fs (FWHM) with a Gaussian fit and  $\sim 25$  fs (FWHM) with a Lorentzian fit for the SH and TH pulses, respectively. The retrieved phases indicate that the UV pulses are nearly transform-limited. As shown in Figs. 3(g) and 3(h), the retrieved spectra of the SH and TH pulses agree well with the measured ones. The fine structures in the retrieved spectra might be understood to be the shot to shot fluctuation of the UV pulses,<sup>16</sup> which was averaged out by the measurement of the spectrometer.

Finally, the validity of the M-XFROG was further confirmed by using a twin retrieval of excitation electric fields FROG (TREEFROG) algorithm,<sup>15</sup> which simultaneously reconstructed the gate function and UV pulse. As shown in Fig. 1(b), the retrieved gate function by the TREEFROG algorithm (solid curve) agrees well with the measured molecular alignment gate function (dashed curve), indicating the reliability and robust of the M-XFROG for UV pulse measurements.

In summary, we have demonstrated that molecular-alignment-gated XFROG is a powerful technique for the measurement of ultrashort UV pulses. It differs from the conventional nonlinear frequency mixing process based FROG geometries, and shows unique features for ultrashort pulse characterizations.

This work was partly funded by National Natural Science Fund (Grant Nos. 10525416 and 10804032), National Key Project for Basic Research (Grant No. 2006CB806005), and Projects from Shanghai Science and Technology Commission (Grant Nos. 08ZR1407100 and 09QA1402000).

- <sup>1</sup>D. N. Fittinghoff, J. L. Bowie, J. N. Sweetser, R. T. Jennings, M. A. Krumbügel, K. W. DeLong, R. Trebino, and I. A. Walmsley, *Opt. Lett.* **21**, 884 (1996).
- <sup>2</sup>A. J. Taylor, G. Rodriguez, and T. S. Clement, *Opt. Lett.* **21**, 1812 (1996).
- <sup>3</sup>R. Trebino, K. W. DeLong, D. N. Fittinghoff, J. N. Sweetser, M. A. Krumbügel, and B. A. Richman, *Rev. Sci. Instrum.* **68**, 3277 (1997).
- <sup>4</sup>J. M. Dudley, L. P. Barry, P. G. Bollond, J. D. Harvey, R. Leonhardt, and P. D. Drummond, *Opt. Lett.* **22**, 457 (1997).
- <sup>5</sup>R. Trebino and D. J. Kane, *J. Opt. Soc. Am. A* **10**, 1101 (1993).
- <sup>6</sup>D. J. Kane and R. Trebino, *IEEE J. Quantum Electron.* **29**, 571 (1993).
- <sup>7</sup>K. W. DeLong, R. Trebino, J. Hunter, and W. E. White, *J. Opt. Soc. Am. B* **11**, 2206 (1994).
- <sup>8</sup>T. Tsang, M. A. Krumbügel, K. W. DeLong, D. N. Fittinghoff, and R. Trebino, *Opt. Lett.* **21**, 1381 (1996).
- <sup>9</sup>J. N. Sweetser, D. N. Fittinghoff, and R. Trebino, *Opt. Lett.* **22**, 519 (1997).
- <sup>10</sup>S. Linden, H. Giessen, and J. Kuhl, *Phys. Status Solidi B* **206**, 119 (1998).
- <sup>11</sup>S. Linden, J. Kuhl, and H. Giessen, *Opt. Lett.* **24**, 569 (1999).
- <sup>12</sup>H. Stapelfeldt and T. Seideman, *Rev. Mod. Phys.* **75**, 543 (2003).
- <sup>13</sup>J. Wu, H. Cai, P. Lu, X. Bai, L. Ding, and H. Zeng, *Appl. Phys. Lett.* **95**, 221502 (2009).
- <sup>14</sup>J. Wu, H. Cai, Y. Tong, and H. Zeng, *Opt. Express* **17**, 16300 (2009).
- <sup>15</sup>K. W. DeLong, R. Trebino, and W. E. White, *J. Opt. Soc. Am. B* **12**, 2463 (1995).
- <sup>16</sup>X. Gu, L. Xu, M. Kimmel, E. Zeek, P. O'Shea, A. P. Shreenath, R. Trebino, and R. S. Windeler, *Opt. Lett.* **27**, 1174 (2002).